Asian Journal of Chemistry; Vol. 33, No. 11 (2021), 2839-2844

ASIAN JOURNAL OF CHEMISTRY

https://doi.org/10.14233/ajchem.2021.23398

Synergetic Effects of Temperature and Perpendicular Magnetic Field on Zn-Ni Alloy Electrodepositing Process

N. BENACHOUR[1,2,*], S. CHOUCHANE[2] and J.P. CHOPART[3]

[1]Department of Chemistry, Faculty of Science, University of 20th August 1955, Skikda, Algeria
[2]Department of Chemistry, Faculty of Science, University of Badji Mokhtar, Annaba, Algeria
[3]Laboratoire Ingénierie et Sciences des Matériaux, LISM EA 4695, 21 rue Clément ADER, 51685 REIMS Cedex 2, France

*Corresponding author: E-mail: naimabenachour2018@gmail.com

Received: 2 July 2021; *Accepted*: 16 September 2021; *Published online*: 20 October 2021; AJC-20572

The zinc-nickel alloys were electrodeposited on stainless steel substrates during a chloride acid bath. The electroplating processes were investigated under a moderate perpendicular magnetic flux at uncommon temperatures. The coatings obtained were characterized by scanning microscopy (SEM) including EDX and X-ray diffraction (XRD). Chronopotentiometric curves were additionally implemented for electrochemical analysis. Structural analysis revealed that the obtained alloys consisted of a mix of the homogeneous phase γ-Ni_3Zn_{22} and α-Zn-Ni at 70 ºC. The alloys variations observed within the chemical composition, crystallographic phases and morphology of the alloys. It is often explained particularly, by the progressive hydrogen reaction and therefore the evolution of the adsorbed intermediate species. The synergetic effect was significant at 70 ºC within the 1T field, including the appearance of normal co-deposition.

Keywords: Zinc-nickel, Electrodeposition, Perpendicular magnetic field, Temperature.

INTRODUCTION

Electroplating is an industrial activity that has been practiced for quite 150 years [1]. The electrodepositing of Ni-Zn alloy from aqueous solutions is assessed as an anomalous co-deposition consistent with the Brenner definition [2]. Zinc-nickel alloy coatings are frequently obtained from alkaline or acidic baths [3]. The deposition temperature is one among the foremost important factors within the electroplating of alloys because it's directly dependent on the composition, structure and properties of the alloys [3,4]. The rate deposition is temperature-dependent because the diffusion of metal ion from the electrolyte to the cathode is accelerated by the rise in temperature in most cases [5,6].

According to Qiao *et al*. [7] structural changes are induced by the deposition temperature. They have shown that normal and anomalous co-deposition of Zn-Ni alloys are often performed during the variation of the deposition temperature under specific galvanostatic conditions. On the other hand, the effect of the geometrical configuration of the working electrode is important because the magneto-hydrodynamic effect called MHD depends on the current lines to the B-field orientations [8]. A magnetic field influences the overall mechanisms of electroplating which might explain the modifications induced on the electrochemical processes observed experimentally on the varied properties (texture, structure) also as on the morphology [9]. The magnetic flux significantly modifies X-ray diffraction patterns. It's going to be noted that the preferential orientations (101) and (002) of the zinc phase and (330) γ-Ni_5Zn_{21} phase are favoured to exist in both parallel and perpendicular B [10]. It is, therefore, one of the possible methods for producing better properties during the co-deposition process [11]. However, consistent with Koza *et al*. [12], no significant changes were found when applying a perpendicular magnetic flux, apart from hydrogen desorption.

On the opposite hand, Devos *et al*. [13] & Msellak *et al*. [14] showed that the magnetic field didn't influence the nucleation itself, but the expansion rate of the seeds and their shape. Devos *et al*. [13] also reported that a magnetic flux can change the surface morphology and preferred orientation of nickel grain, due to a rise within the diffusion flux of specific inhibitory species. Moreover, Rabah [15] found that the perpendicular

magnetic flux affects the deposit composition. The method suggested that the surface diffusion of adatoms might be influenced by the B field [16]. This study shows the temperature effect on the deposition under a moderate magnetic field; which is applied perpendicularly to the electrode surface to attenuate the MHD effects. The objective of this article is to investigate the temperature effects on the structure of Zn-Ni alloys under a perpendicular magnetic flux. The various structures were at various temperatures within the absence of magnetic flux. The experiments were then, repeated under the magnetic flux for testing the possible synergetic effects which provide a normal co-deposition; when the deposition of nickel is preferentially in many cases, at the same time it's possible to get deposits, which will be used as metallic coatings for corrosion protection.

EXPERIMENTAL

The used electrolytic solution contains H_3BO_3: 0.1 M, $ZnCl_2$: 1.8 M, $NiCl_2 \cdot 6H_2O$: 1.1 M. The substrates were stainless steel plates with a surface of 1 cm^2 to obtain good reproducibility of the experiments. The surface of the electrode was polished before each deposit by respecting the subsequent steps: polishing of the surface with the glass paper p # 1200 until # 4000 then polishing with a felt ESCIL with a suspension of alumina with a grain size of 1 µm and eventually washing with distilled water. The pH of solution was 4.86. The studied temperatures at 30, 40, 50, 60 and 70 ºC were regulated by a thermostated double-walled glass cell, placed into a gap of an electromagnet (DRUSLH EAM20G), which may deliver a magnetic flux of amplitude up to 1.1 T. The electrochemical cell was connected to a potentiostat, voltalab201, controlled by a software voltamaster 4 and therefore the current density applied was -20 mA/cm^2. The X-ray diffraction investigations of deposits was carried out using the BRUKER D8 ADVANCED X-Ray diffractometer equipped with copper anticathode (Cu$K\alpha$ = 1.54056 Å). The morphology and chemical composition were identified by a JEOL JSM 6460LA microscope including an EDS JEL 1300 microprobe.2.

RESULTS AND DISCUSSION

Chronopotensitometric curves: The Zn-Ni co-deposits in absence and the magnetic field presence for two intensities, B = 0.5 and 1 T in a temperature range of 30 to 70 ºC were investigated in order to review the synergy between these two parameters (Fig. 1).

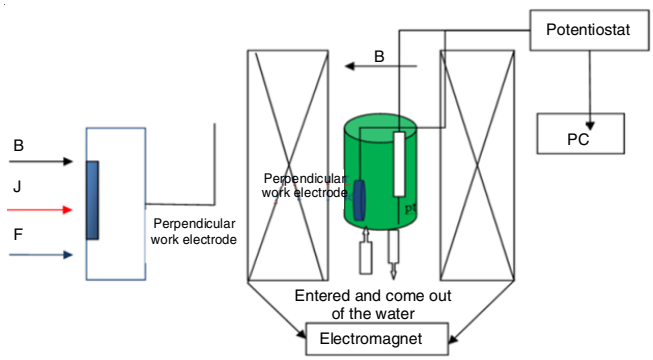

Fig. 1. Experimental setup

In first case (Fig. 2a), without the magnetic flux, the curves show a rise in cathode potentials as a function of the increase in temperature. When the temperature increased from 30 to 40 ºC, the cathodic potential varies. From 40 to 60 ºC, no significant variation was observed, which corresponds to the natural convection. However, a rise that becomes significant at 70 ºC. These differences observed between the curves obtained may correspond to a difference in reduction kinetics, depending on the expected deposition temperature, which accelerates the diffusion of the ions. Hence, the reaction was faster at 70 ºC. The increase in plateau potential values, necessary to create the initial nucleus; consequently, more nickel was deposited. Therefore, Qiao [7] found that the high current efficiency for zinc-nickel co-deposition decreases when the depositing temperature is above 40 ºC. This decrease in current efficiency was due to improved hydrogen evolution. Qiao [7] also verified that the cathodic potential notation is increased in the presence

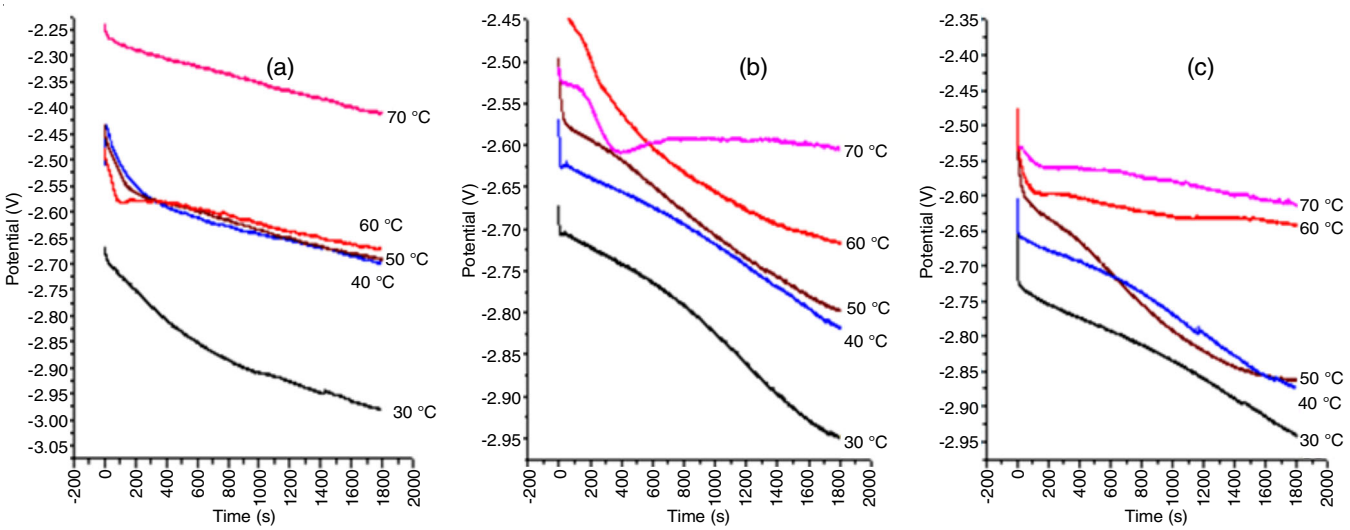

Fig. 2. Chronopotentiometric curves during the process of electroplating: (a) without field, (b) (0.5T), (c) (1T) for temperatures 30, 40, 50, 60 and 70 °C

of high nickel content in zinc-nickel alloy coatings. When a magnetic field was applied for an amplitude of B = 0.5 T (Fig. 2b), a considerable variation of the potential can be noticed. At 70 ºC, there is a sharp drop in potential towards -2.6 V, which corresponds to the double-layer charge at the beginning of the electroplating process and then the deposition takes place. Generally, within the initial stages of deposition, a decrease in potential was observed for all B intensities, which revealed the charge transfer that takes place at the beginning of electroplating process. It can be noticed that the charge time was more significant during this case (contrary to B = 0 T). Iwakura *et al.* [17,18] attributed this phenomenon to the hydrodynamic effect due to mixed convection. This might even be due to the variation of nickel content within the coating. Therefore, it can be assumed that the changes of nickel content in the deposit are often closely associated to the evolution of the cathodic potential, since the temperature change because the metal ion diffusion from the electrolyte to the cathode is increased [7]. The enlargement of the E-t curves at a lower time shows a rounded shape, which indicates the presence of an adsorption process, probably associated with an intermediate (ZnNiad) [19,20].

On the other hand, at B = 1 T (Fig. 2c), the difference between the 30 and 70 ºC curves is reduced, which may be attributed to a synergy between the convective effect of the magnetic field and the temperature. Matsushima *et al.* [16] suggested that the nucleation rate or deposition tends to be inhibited under the magnetic field; this is often is coherent with the present results. However, during this study, both the magnetic field and the current lines are perpendicular to the electrode surface. In this configuration, no increase within the limiting current generated by Lorentz force is expected since the product J × B is zero. However, consistent with Rabah [15] on paramagnetic systems, the magnetic field allows obtaining a controlled hydrodynamic regime at (B = 1 T) of a magnetic field, which is confirmed in the present case.

X-ray diffractions: The identification of the deposit phases is obtained by XRD diffractogram. Various phases were observed altogether cases. Firstly, some crystal structure variation can be observed without a magnetic field and for all temperatures studied (40, 50, 60, 70 ºC); (Fig. 3a) initially, at 30 ºC, the composition γ-Ni_3Zn_{22} with an orientation (330) is visible at 43º, then at 40 ºC, the peak 2θ = 43.7º widens the corresponding phase γ-Ni_3Zn_{22} (113), which intensifies at 50, 60 and 70 ºC. It is known that in ZnNi; the γ-(330) phase was usually present with variable intensity and depends on the coating [22].

Therefore, an intense peak around 2θ = 43.3º at 60 and 70 ºC was observed, corresponding to β-NiZn (101). It is also noticed the appearance of a new peak at 70 ºC near 35.3º, which corresponds to the composition Ni_3Zn_{22} (022). Gou & Sun [23] found the composition β-NiZn in alloys containing about 50% zinc atoms. The XRD patterns obtained from the deposits prepared at B = 0.5 T show (Fig. 3b) that at 30 °C an intense peak corresponds to zinc the composition γ-Ni_3Zn_{22} (330). In addition, an equivalent result's observed clearly at 40 ºC, this peak is a smaller amount intense for 50 and 60 ºC. The main difference between Zn-Ni diffractogram was observed on deposits developed under 60 and 70 ºC, where a new reflection appears around 35.2º, which corresponds to the composition α-Ni_3Zn_{22} (022). Fig. 3b shows that γ-Ni_3Zn_{22} phase with the preferred orientation (330) was usually preferred within the temperature range of 30 to 50 ºC under B = 0.5 T. However, at 60 ºC, the X-ray pattern revealed the significant peaks, suggesting that the deposit is almost amorphous. The disappearance of γ-Ni_3Zn_{22} (330) was observed at 70 ºC.

The generation of composition α-NiZn (101) is also observed. Fratesi & Roventi [24] observed that when the nickel content in the Zinc-Nickel alloy coating was greater than 50%, the γ phase disappeared. The diffraction patterns of Zn-Ni deposits obtained under B = 1T for an equivalent temperature range are shown in Fig. 3c. A peak near 42.8º is characterized by γ-Ni_2Zn_{11} (330). A new peak appearing around 2θ = 35º at 30 and 40 ºC corresponds to the α-Ni_3Zn_{22} (022) phase at 70 ºC. The formation of α-NiZn homogeneous phase with orientation (101) is additionally observed. It is also observed that the peaks at 43º are slightly broadened and intensify with increasing temperature. The broadening of the peck must be attributed to crystal size reduction; broader pecks characterize smaller crystallites. This remark becomes visible for crystallites less than 1 µm in diameter. The peak intensity is highest at B = 1 T, which was observed at 60 and 70 ºC. However at 70 ºC, the αNiZn phase was formed [23]. Besides, the magnetic field always favours the orientation (101) of the zinc phase. It also prefers zinc and therefore the η phase [25] but during this study, the Zn-Ni alloys obtained have two main phases: the homogeneous γ-Ni_3Zn_{22} phase with an (330) orientation and therefore the α-Zn-Ni phase (101), which appears at 70 ºC within the presence and absence of a magnetic flux. Alfantazi

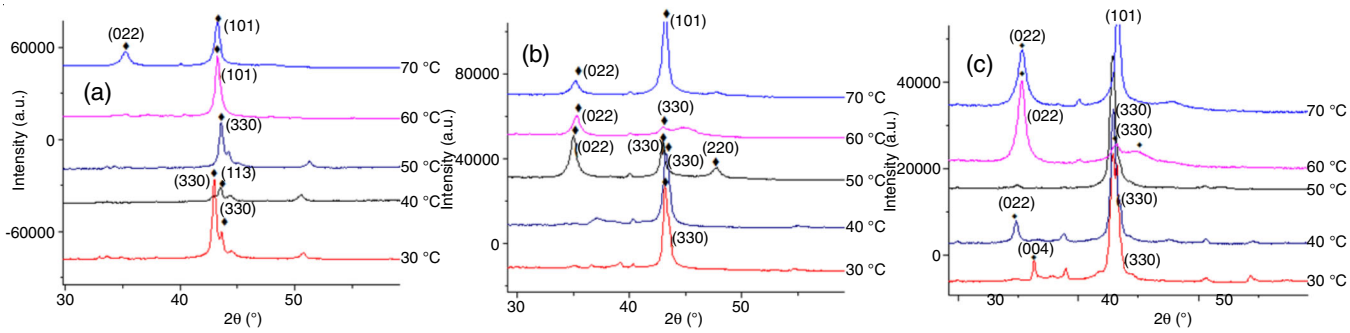

Fig. 3. X-ray diffraction patterns of the electrodeposits Zn–Ni alloy under: a (B = 0T), b (0.5T), c (1T) and at temperatures 30, 40, 50, 60 and 70 °C

et al. [26] observed that the phase α-structure is that the only phase present in zinc-nickel coatings with a nickel content of 63%. Furthermore, the phase changes and texture variations remarked in the presence of the magnetic field are a consequence of the convection phenomenon induced by magneto-hydrodynamic effects and temperature. In addition, the magnetic field generates a rise within the Ni ions diffusion towards the cathode because the rate of nickel electroplating from a concentrated solution is under kinetic control [27]. It can be concluded that the solid solution of Ni (Zn) α was formed in deposits above 50 ºC, which is coherent with of the mechanism instantaneous nucleation. In other concept, Zn forms a substituted solid solution by replacing the Ni atom within the FCC lattice [28].

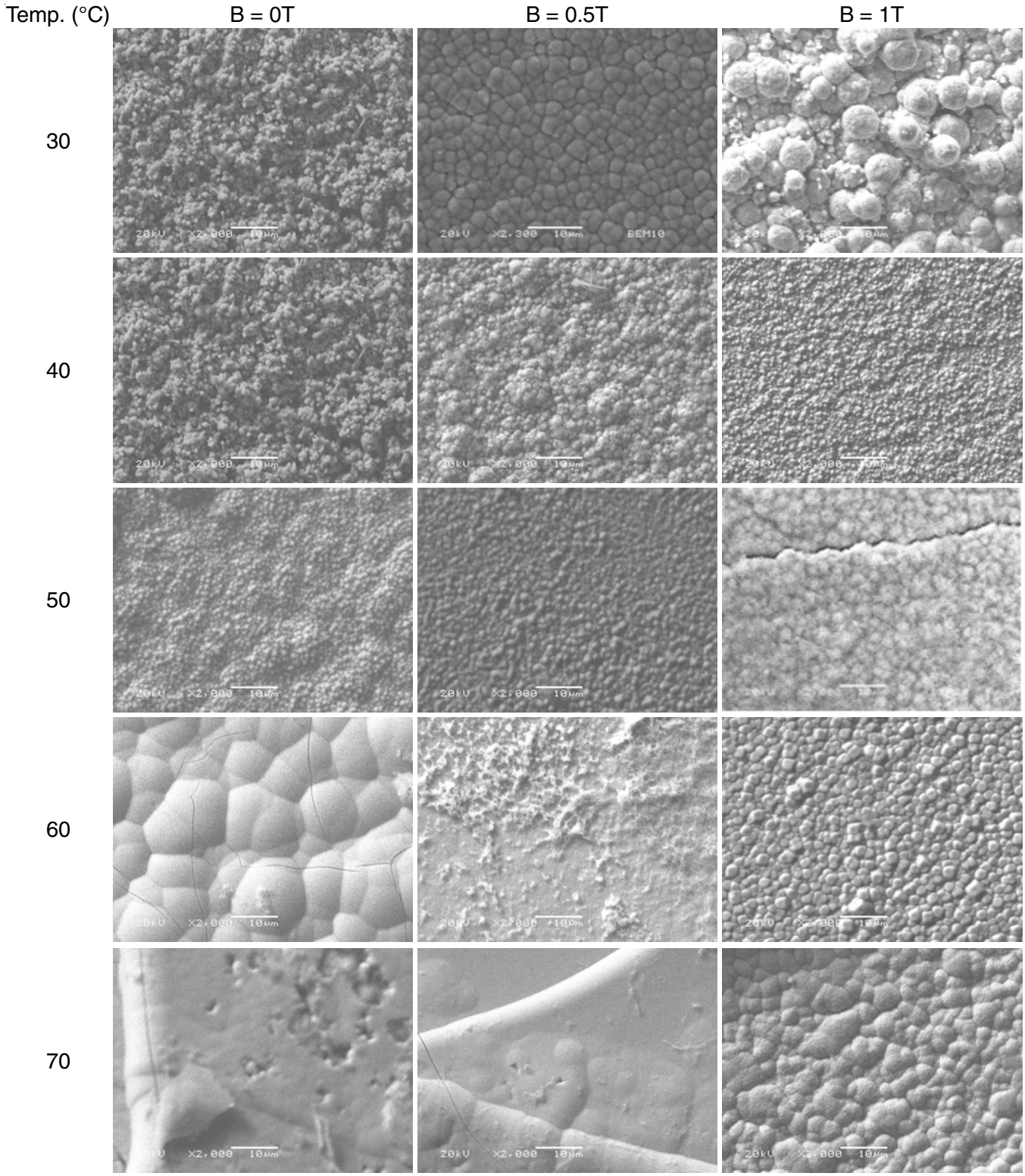

Fig. 4. SEM images showing the morphology of the deposits obtained in studied cases; B = 0T, B = 0.5T and B = 1T

SEM studies: In this work, SEM characterization shows that the morphology of the deposit surfaces varies with the temperature variations. In the absence of field, a slight variation in grain size and morphology are often observed around 1 µm. Hence, the images corresponding to temperatures of 30, 40 and 50 ºC show nodule grains of varied sizes due to of the increased temperature of the zinc-nickel deposit, these results indicate good coatings with a compact morphology [7,29].

In present case, a pronounced change in surface morphology accompanied by nodular grains and fissures was observed above 60 ºC. The deposits are degraded with the appearance of cracks, which can been attributed due to the presence of hydrogen atoms [30]. The morphological structure of the deposits above 60 ºC is varied and not crystallite, but flat. Eliaz *et al*. [31] showed that at elevated temperatures, the desorption mechanism is more important than increasing the active surface area. Therefore, this surface is available for the hydrogen evolution reaction and causes the formation of hydroxide ions.

The same result's observed for alloys obtained under B = 0.5 T; the temperature refines the crystallites retaining a size of 1.5 µm at 50 ºC. On the other hand, the alloy presents a granular morphology and a particularly small grain size. These results are following by the work of Roventi *et al*. [32]. Therefore, under this moderate magnetic field intensity; no cracks are observed and the alloy morphology also appears compact. Under an intensity of B = 1 T and at 60 and 70 ºC; a disappearance of the visible cracks is observed, which can be attributed to the desorption of hydrogen, caused by the perpendicular field [12]. However, it is also observed the appearance of cracked dimensional dendrites at 50 ºC. On the other hand, at 30 ºC, a three-dimensional spherical form is observed; which indicates the mass transport controlled electrocrystallization process [12].

However, at a higher intensity of B (1T), the resulting coating was more porous due to the excessive evolution of the hydrogen reaction. It were often noted that each one alloys obtained at 1T have a light grey colour and globular morphology with different grain sizes (Fig. 4). It can be concluded that the perpendicular magnetic field modifies to some measure the depositing mechanism that may perform Zn-Ni alloys with good physical properties.

EDX measurements: Fig. 5a-c summarizes the chemical composition of Ni-Zn deposits, as determined by EDXS, as a function of deposition temperature and magnetic field. In Fig. 5a, without the magnetic field a rise within the percentage of Ni between 30 and 50 ºC was observed. This increase causes a significant decrease in the content of Zn within the deposit, confirmed that the higher temperature favours the deposition of Ni consistent with the work of Roventi *et al*. [32]. However, the evolution of nickel composition is slight between 60 and 70 ºC during this study. In addition, Fig. 5b shows the effect of both parameters: temperature and magnetic flux (B = 0.5T). The nickel content increases in the same manner as within the absence of a magnetic field. However, up to 70 ºC, a increase from 30.67 to 63.42 Ni wt.% between 60 and 70 ºC was observed. This increase appears to be strong when a field of 1T (Fig. 5c) was applied which rises to 77.29 Ni wt.%. This result verified that the marked increase in the nickel content above 60 ºC due to the presence of B. Sometimes, this phenomenon has been attributed to the transition from an anomalous to a normal deposition [33]. According to the results (Fig. 5), it is concluded that the rise in nickel composition is proportional to extend in temperature. The nickel composition variation of the coating confirms the convective synergy effect, of the perpendicular magnetic flux and therefore, the temperature at 70 °C is more significant at an intensity of 1T. It can be deduced that the Ni content features a significant influence on the morphology and grain size of coatings, similar result has been found by other workers also [35].

Conclusion

In present study, the zinc-nickel alloys were electrodeposited on stainless steel substrates in a chloride acid bath. The influence of temperature in the perpendicular magnetic field has a strong influence on the structure, grain size and surface morphology of Zn–Ni alloy deposits. It was also observed that the field-effect on the cathode potential evolution was negligible at 30 ºC. However, this effect becomes more and more important in temperature function particularly at 70 ºC. From the X-rays diffraction analysis, it can be concluded that α-Ni (Zn) was formed in the deposits at 70 ºC with the appearance of α-Ni_3Zn_{22} (022). The broadening of some peaks should be attributed to the reduced crystal size. Moreover, a remarkable changes in the morphology's evolution as a function of temperature above 60 °C were also noted. A large increase in the nickel content occurs at 70 ºC and 1T, which was attributed to a convective magnetic field synergy and temperature.

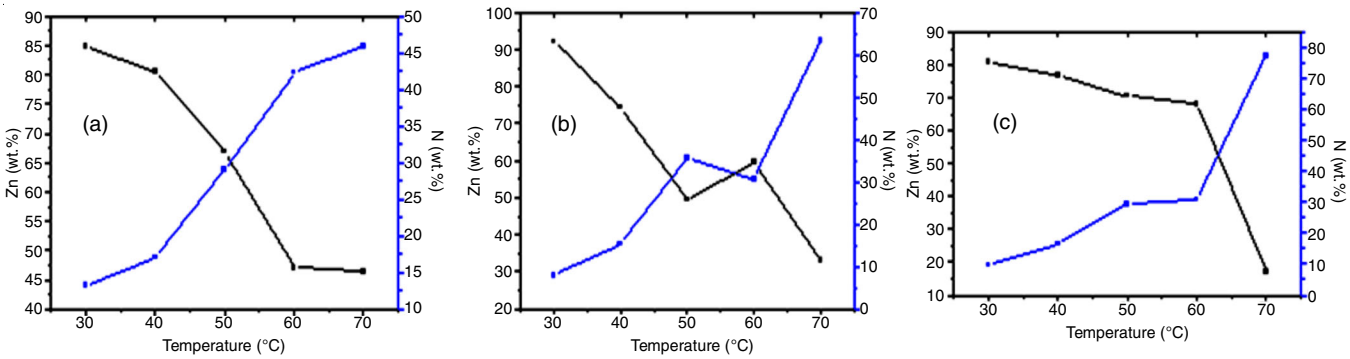

Fig. 5. Evolution of the composition of the Zn-Ni deposit as a function of the temperatures studied in the three cases; a (0T), b (0.5T), c (1T). (Based on EDX measurements)

CONFLICT OF INTEREST

The authors declare that there is no conflict of interests regarding the publication of this article.

REFERENCES

1. O.S.I. Fayomi, I.G. Akanade and A.A. Sode, *J. Phys.: Conf. Ser.*, **1378**, 042084 (2019); https://doi.org/10.1088/1742-6596/1378/4/042084
2. C.M. Praveen Kumar, A. Lakshmikanthan, M.P.G. Chandrashekarappa, D.Y. Pimenov and K. Giasin, *Coatings*, **11**, 712 (2021); https://doi.org/10.3390/coatings11060712
3. H.Y. Lee and S.G. Kim, *Surf. Coat. Technol.*, **135**, 69 (2000); https://doi.org/10.1016/S0257-8972(00)00731-3
4. S.N. Srimathi and S.M. Mayanna, *Metal Finishing*, **11**, 35 (1985).
5. L.C. Li, Y. Zhang, S. Deng and Y. Chen, *Mater. Lett.*, **57**, 3444 (2003); https://doi.org/10.1016/S0167-577X(03)00097-1
6. F.J.F. Miranda, O.E. Barcia, O.R. Mattos and R. Wiart, *J. Electrochem. Soc.*, **144**, 3449 (1997); https://doi.org/10.1149/1.1838031
7. X. Qiao, H. Li, W. Zhao and D. Li, *Electrochim. Acta*, **89**, 771 (2013); https://doi.org/10.1016/j.electacta.2012.11.006
8. A. Levesque, S. Chouchane, J. Douglade, R. Rehamnia and J.-P. Chopart, *Appl. Surf. Sci.*, **255**, 8048 (2009); https://doi.org/10.1016/j.apsusc.2009.05.012
9. V.R. Rao, K.V. Bangera and A.C. Hegde, *J. Magn. Magn. Mater.*, **345**, 48 (2013); https://doi.org/10.1016/j.jmmm.2013.06.014
10. S. Chouchane, Ph.D. Thesis, Electroplating of Zn-Ni Alloys: Effects of a Magnetic Field on their Compositions and Properties, University of Reims URCA (2008).
11. S. Chouchane, A. Levesque, J. Douglade, R. Rehamnia and J.-P. Chopart, *Surf. Coat. Technol.*, **201**, 6212 (2007); https://doi.org/10.1016/j.surfcoat.2006.11.015
12. J.A. Koza, M. Uhlemann, A. Gebert and L. Schultz, *Electrochim. Acta*, **53**, 5344 (2008); https://doi.org/10.1016/j.electacta.2008.02.082
13. O. Devos, A. Olivier, J.P. Chopart, O. Aaboubi and G. Maurin, *J. Electrochem. Soc.*, **145**, 401 (1998); https://doi.org/10.1149/1.1838276
14. K. Msellak, Ph.D. Thesis, Metal Electroplating under MHD control: Physical and Electrochemical Characterization, University of Reims, URCA (2003).
15. L. Rabah, Ph.D. Thesis, Convection by Magnetic Susceptibility Gradient: Effects on the Electrodeposition of Copper and Cobalt-Iron Alloy, University of Reims URCA (2007).
16. H. Matsushima, A. Ispas, A. Bund and B. Bozzini, *J. Electroanal. Chem.*, **615**, 191 (2008); https://doi.org/10.1016/j.jelechem.2007.12.010
17. C. Iwakura, T. Edamoto and H. Tamura, *Denki Kagaku*, **52**, 596 (1984); https://doi.org/10.5796/kogyobutsurikagaku.52.596
18. C. Iwakura, T. Edamoto, H. Tamura, *Denki Kagaku*, **52**, 654 (1984); https://doi.org/10.5796/kogyobutsurikagaku.52.654
19. O. Aaboubi, A. Hadjaj and A.-Y. Ali Omar, *Electrochim. Acta*, **184**, 276 (2015); https://doi.org/10.1016/j.electacta.2015.10.054
20. G. Roventi, R. Fratesi, R.A.D. Guardia and G. Barucca, *J. Appl. Electrochem.*, **30**, 173 (2000); https://doi.org/10.1023/A:1003820423207
21. E. Chassaing and R. Wiart, *Electrochim. Acta*, **37**, 545 (1992); https://doi.org/10.1016/0013-4686(92)87047-4
22. Z.A. Mahmud, F. Amelotti, C. Serpi, J, Maskaric, M. Mirabal, N. Mingolo, L. Gassa, P. Tulio and G. Gordillo, *Proced. Mater. Sci.*, **9**, 377 (2015); https://doi.org/10.1016/j.mspro.2015.05.007
23. S.-P. Gou and I.-W. Sun, *Electrochim. Acta*, **53**, 2538 (2008); https://doi.org/10.1016/j.electacta.2007.10.039
24. R. Fratesi and G. Roventi, *J. Appl. Electrochem.*, **22**, 657 (1992); https://doi.org/10.1007/BF01092615
25. S. Chouchane, A. Levesque, P. Zabinski, R. Rehamnia and J.-P. Chopart, *J. Alloys Compd.*, **506**, 575 (2010); https://doi.org/10.1016/j.jallcom.2010.07.099
26. A.M. Alfantazi, G. Brehaut and U. Erb, *Surf. Coat. Technol.*, **89**, 239 (1997); https://doi.org/10.1016/S0257-8972(96)02894-0
27. I. Epelboin, M. Jousselin and R. Wiart, *J. Electroanal. Chem.*, **119**, 61 (1981).
28. H.Y. Yang, X.W. Guo, X.B. Chen, S.H. Wang, G.H. Wu, W.J. Ding and N. Birbilis, *Electrochim. Acta*, **63**, 131 (2012); https://doi.org/10.1016/j.electacta.2011.12.070
29. M. Kwon, D. Jo, S.H. Cho, H.T. Kim, J.-T. Park and J.M. Park, *Surf. Coat. Technol.*, **288**, 163 (2016); https://doi.org/10.1016/j.surfcoat.2016.01.027
30. S.S.A. El Rehim, E.E. Fouad, S.M.A. El Wahab and H.H. Hassan, *Electrochim. Acta*, **41**, 1413 (1996); https://doi.org/10.1016/0013-4686(95)00327-4
31. N. Eliaz, K. Venkatakrishna and A.C. Hegde, *Surf. Coat. Technol.*, **205**, 1969 (2010); https://doi.org/10.1016/j.surfcoat.2010.08.077
32. G. Roventi, R. Cecchini, A. Fabrizi and T. Bellezze, *Surf. Coat. Technol.*, **276**, 1 (2015); https://doi.org/10.1016/j.surfcoat.2015.06.043
33. F. Elkhatabi, M. Benballa, M. Sarret and C. Müller, *Electrochim. Acta*, **44**, 1645 (1999); https://doi.org/10.1016/S0013-4686(98)00286-2
34. Z. Feng, Q. Li, J. Zhang, P. Yang, H. Song and M. An, *Surf. Coat. Technol.*, **270**, 47 (2015); https://doi.org/10.1016/j.surfcoat.2015.03.020